Journal of Hydrology 566 (2018) 137–149

Contents lists available at ScienceDirect

Journal of Hydrology

journal homepage: www.elsevier.com/locate/jhydrol

Research papers

Groundwater-flow characterization in a multilayered karst aquifer on the edge of a sedimentary basin in western France

Guillaume Lorette*, Roland Lastennet, Nicolas Peyraube, Alain Denis

University of Bordeaux, I2M-GCE-CNRS 5295, Pessac, France

ARTICLE INFO

This manuscript was handled by C. Corradini, Editor-in-Chief, with the assistance of Dongmei Han, Associate Editor

Keywords:
Multilayered karst aquifer
Hydrochemistry
Hydrodynamic
Hydrogeology

ABSTRACT

On the edge of sedimentary basins, burial of geological layers can involve the formation of confined karst aquifers. In some cases, relationships between confined and unconfined karst aquifers can exist and imply an increased difficulty in delineating contributive areas of karst system outlets with accuracy. This work aims to develop a multi-disciplinary approach to highlight groundwater exchanges between multilayered karst aquifers feeding a single spring.

Toulon Springs, located in western France, provides the opportunity to study relationships between two multilayered karst aquifers. Hydrograph and chemograph analysis coupled with principal component analysis (PCA) are used to evaluate groundwater-flow origins on the northern edge of a sedimentary basin. Natural hydrodynamic responses (baseflow recession analysis, auto-cross correlation function) show an important volume of water located in a saturated zone of the Toulon karst system. Significant contrasts in water quality as a function of the hydrological regime (flood, recession, and baseflow regime) and comparison with shallow and deep water show the participation of a deep aquifer supporting the flow of Toulon Springs.

1. Introduction

Karst aquifers are one of the most important water supply sources worldwide. Approximately 25% of the world's population consumes water obtained from karst aquifers (Ford and Willians, 2007). These complex systems have a high degree of heterogeneity that distinguish them from other aquifers (White, 1988; Bakalowicz, 1995, 2005; Ford and Willians, 2007; Worthington and Ford, 2009).

Analysis of karst systems is usually led using several methods based on classical chemistry, isotopic chemistry, hydrodynamic responses, or some lithology characteristics of carbonates. The joint use of hydrodynamic and hydrochemical techniques, within the framework of a multidisciplinary approach, provides a reliable characterization of the hydrogeological functioning of karst aquifers (Lastennet and Mudry, 1997; Grasso et al., 2003; Perrin et al., 2003; Birk et al., 2004; Bicalho et al., 2012, Brkic et al., 2018, Filippini et al., 2018). Hydrochemical and hydrodynamic responses observed at the outlet of karst systems depend upon the flow conditions that prevail in the aquifer. Previous studies (Lastennet, 1994; Lastennet and Mudry, 1997, Raeisi and Karami, 1997; Emblanch et al., 1998; Batiot et al., 2003a; Batiot et al., 2003b; Emblanch et al., 2003; Doctor et al., 2006; Mudarra and Andreo, 2011; Nicolini et al., 2016) have focused on the joint use of natural hydrochemical tracers such as dissolved organic carbon (D.O.C.), nitrates (NO_3^-), or magnesium (Mg) to improve the knowledge about the functioning of these karst systems. Most of karst studies tried to apply their methods on springs fed by a single karst aquifer.

The geological history of the edge of sedimentary basins can lead to the formation of multilayered aquifers through the progressive burial of geological layers. This burial involves the passage of unconfined aquifers to confined aquifers of some layers. The succession of periods of regression-transgression implies several karstification phases. This involves complex relationships between unconfined and confined multilayered aquifers. In some cases, a karst spring can act as the outlet for both of these multilayered aquifers. This implies complex hydrodynamic and hydrochemical responses at the spring and an increased difficulty in accurate delineation of limits of the karst system. The recharge of these multilayered karst aquifers is a major issue for the edge of sedimentary basins. Few studies focus their attention on karst springs fed by several aquifers. We can note insights from the work of Bicalho et al. (2012) or Mahler and Bourgeais (2013). Recent studies have proposed several polyphased karstification concepts in relation to both epigene and hypogene karstification (Klimchouk, 2007, 2012; Palmer 2011; Audra et al., 2015; Husson et al., 2016).

The site of Toulon Springs is a good example of a complex karst system drained by two multilayered karst aquifers from Jurassic and Cretaceous aquifers, located on the northern edge of the Aquitaine

* Corresponding author at: University of Bordeaux, I2M-GCE-CNRS 5295, Allee Geoffroy Saint-Hilaire, Bât. B18, 33600 Pessac, France.
E-mail address: lorette.guillaume@gmail.com (G. Lorette).

https://doi.org/10.1016/j.jhydrol.2018.09.017
Received 27 April 2018; Received in revised form 7 September 2018; Accepted 8 September 2018
Available online 10 September 2018

sedimentary basin (66 000 km^2). Polyphased karstification concepts are directly linked to the geological history of the Aquitaine basin (Pelissié, 1982; Platel, 1987; Cubaynes et al., 1989; Rey et al., 1988; Pélissié and Astruc, 1996). Toulon Springs have been supplying water to the metropolitan area of Périgueux (Dordogne county, France) since the 19th century. Previous works (Von Stempel, 1972; Lastennet et al., 2004; Lorette et al., 2016) have led to the first studies but have left questions about the functioning and groundwater origins of Toulon Springs. Toulon Springs provide the opportunity to understand the functioning of a multi-reservoir karst aquifer using simple acquisition of hydrodynamic responses and natural hydrochemical tracers. Geochemical monitoring of several karst springs allows for Toulon Springs to be placed into a local hydrogeological situation and to identify the different aquifers participating in the feeding of Toulon Springs. Particular attention is given to the origins of magnesium and to the relationship between magnesium concentration and dissolved oxygen concentration in both confined and unconfined karst aquifers. (Emblanch et al., 1998; Batiot et al., 2003a; Mahler and Bourgeais, 2013) previously discuss these parameters. Because of the close connection with the surface and short travel times, groundwater in many karst aquifers is oxic (Perrin et al., 2007; Mahler et al., 2011; Musgrove et al., 2011). In some cases, the dissolved oxygen concentration can decrease, associated with increased magnesium concentration. This information is linked to residence time of water into the aquifer or to a mix of water with several aquifers. It will be discussed in this work.

The main goal of this paper is to use a multidisciplinary approach to determine the groundwater flow-mechanism of a single spring fed by a multilayered karst aquifer, The first objective is to assess the water quantity available into the Toulon karst system using natural hydrodynamic responses. The second one is to assess the water quality using natural hydrochemical responses. The third one is to combine these tools to evaluate the functioning of a typical example of a complex karst system drained by two multilayered karst aquifers located on the northern edge of a sedimentary basin, proposing a conceptual model of functioning.

2. General characteristics of the study area

2.1. Local geology and hydrogeology

Toulon Springs are major regional springs and are located in Périgueux (south-western France, at the northern edge of the Aquitaine sedimentary basin). It is a Vauclusian-type spring, located on a major faulted anticlinal structure, oriented N145 (Lastennet et al., 2004). Toulon Springs are the main perennial outlet of the karst system that can reach almost 1 000 L.s^{-1} during rainfall events, with a mean annual daily discharge of 450 L.s^{-1}.

The geological situation of the Toulon karst system consists of upper Cretaceous and upper Jurassic carbonate rocks (Fig. 1), with a thickness of 200–250 m for Cretaceous rocks and 300–350 m for Jurassic rocks (Kimmeridgian, Oxfordian, Bathonian, Bajocian) (Von Stempel, 1972). At the top, Cretaceous rocks consist of limestone, while Jurassic rocks consist of dolomitic limestone and dolomites. The geological structure of the Toulon karst system is characterized by the existence of folds and fractures in a mainly NW-SE direction (Fig. 1).

Karst landforms are well developed at the surface of the carbonate outcrops, mainly in Cretaceous limestone, as noticed by the existence of dolines and swallow holes.

The regional hydrogeological situation consists of two main multilayered karst aquifers (Fig. 1). Fractured and karstified Cretaceous limestone constitutes the first main aquifer. It is composed of a Turonian aquifer, Coniacian aquifer and Santonian aquifer (Fig. 1). Below, Jurassic dolomitic limestone constitutes the second main aquifer of the study area. It is composed of a Kimmeridgian aquifer, Oxfordian aquifer, Bathonian aquifer and Bajocian aquifer (Fig. 1). The marls of the Cenomanian are considered to be the impermeable limit of these two main aquifers. Spatial thickness variations (4–20 m) and facies variations (marls-sands) over the study area induce an additional difficulty in the understanding of the relationships between the two main aquifers.

Although both of these aquifers are supposedly hydrogeologically isolated, deep water rising occurs from the Jurassic into the Cretaceous through the faulted anticline structure of Périgueux. This deep water rising is illustrated by the presence of many warm springs (between 20 and 21 °C) including COPO spring (Club Olympique de Perigueux Ouest) (Fig. 1), located in the Isle River Valley. The Isle River represents the regional base level of the Toulon karst system.

The hydrogeological catchment of Toulon Springs has an area of approximately 100 km^2 (Fig. 1). A large part of the hydrogeological catchment is relatively permeable, due to the presence of limestone of the Santonian and the Coniacian. Most of the recharge is diffuse through outcrops located by the north of Toulon Springs (Fig. 1). Localized infiltration occurs through sinkholes along the basin. Several tracer tests have been conducted over the past 30 years, leading to the delineation of the catchment area of Toulon Springs (Fig. 1). This area crosses the Beauronne River to the West of the basin. The Beauronne River has sinkholes situated in the main bed that may possibly participate in the recharge of the aquifer. However, during low-water periods, the Beauronne River does not flow.

2.2. Climate

The climate of Périgueux is temperate with an average annual temperature of 13 °C, an average summer temperature between 20 °C and 21 °C, and an average winter temperature between 5 °C and 6 °C. The study area has three rainfall stations and one meteorological station (Fig. 1) in order to cover the whole hydrogeological basin of Toulon Springs. Although the average annual precipitation varies between 800 and 1000 mm, evapotranspiration from vegetation and soil leads to a computed effective rainfall ranging from 200 to 350 mm per year (calculated from the Penman-Monteith equation). Evapotranspiration reaches a peak in July-October, when rainfall is generally insufficient to produce any significant discharge, except during strong storms.

Illustrating by Toulon Springs, the main objective of this work is to understand the hydrogeological functioning of a complex karst system fed by multilayered karst aquifer on the northern edge of a sedimentary basin.

3. Material and methods

The main experimental strategy aims to evaluate the hydrogeological functioning of a Toulon springs. Then, it intends to assess dynamics of the flow during high-water periods and low-water periods, both from a hydrodynamic and hydrochemical point of view. Finally, water samples and *in situ* measurements performed on the study area aim to identify different water types flowing into both Jurassic and Cretaceous karst aquifers.

3.1. Water sampling and data continuous monitoring

At Toulon Springs, water samples were collected semi-monthly from February 2014 to October 2015 and weekly from October 2015 to October 2017, with daily sampling during groundwater flood events. A total of 187 samples were collected from Toulon Springs.

In the field, a multiparameter WTW 3430 was used to measure temperature (T), pH (pH), electrical conductivity (EC) and dissolved oxygen (O2) to a precision of ± 0.1 °C, ± 0.05, ± 1 µS.cm^{-1}, and ± 0.1 mg.L^{-1} respectively. Alkalinity was measured within 12 h, by acid titration at the laboratory I2M-GCE Bordeaux.

High resolution monitoring is perform at Toulon Springs since 2015. The electrical conductivity (EC), turbidity, dissolved organic carbon (DOC), nitrate (NO_3^-), water temperature (T), and dissolved oxygen

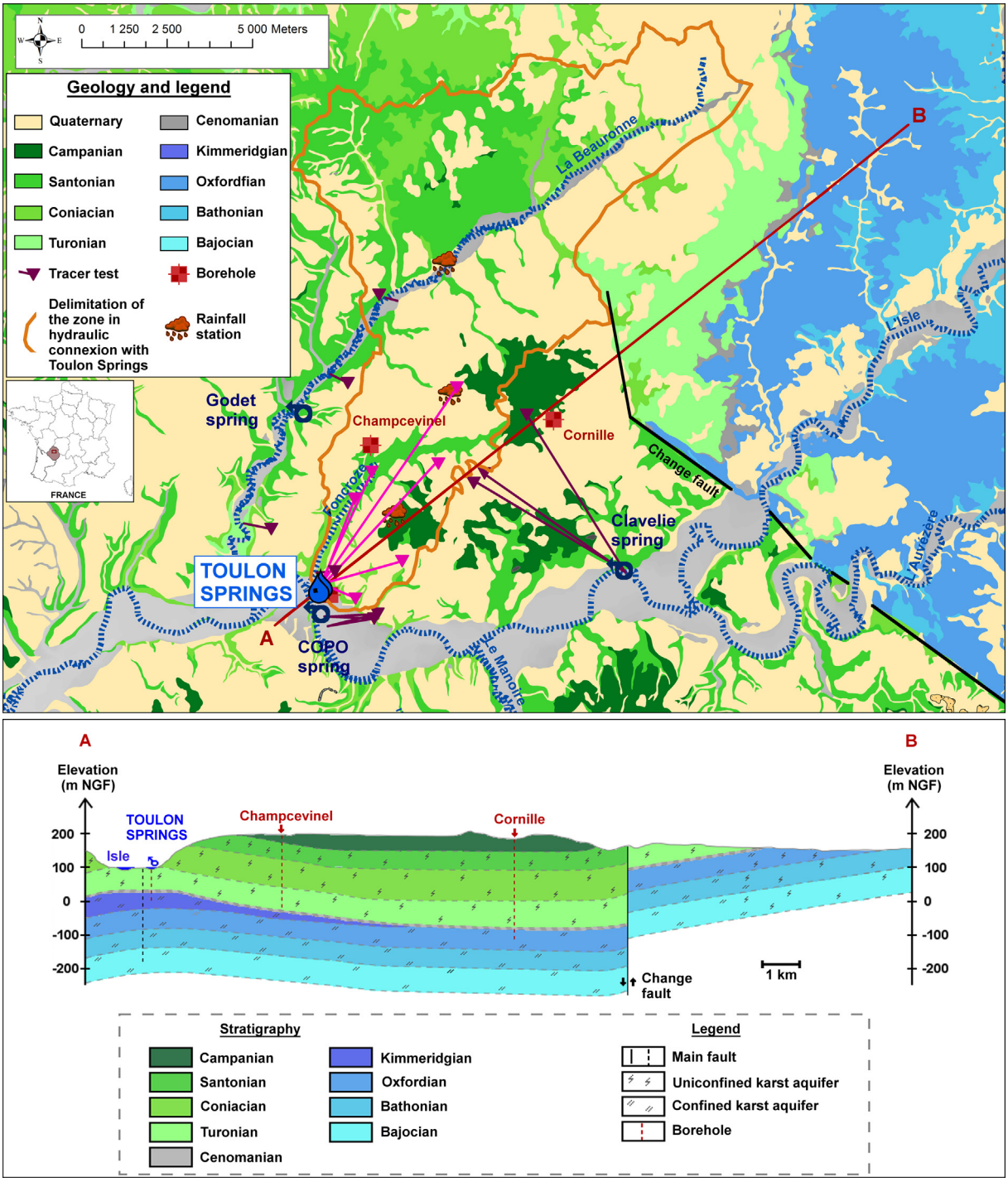

Fig. 1. Hydrogeological map of the Toulon karst system, with sampled springs and rain gauge location. AB: simplified SW-NE geological cross-section. The Cenomanian is considered as not aquifer.

(O2) are recorded every 10 min with an accuracy of ± 1 µS.cm^{-1}, ± 0.02 NTU, ± 0.02 mg.L^{-1}, ± 0.05 mg.L^{-1}, ± 0.1 °C, ± 0.05 mg.L^{-1}, respectively. Finally, discharge is measured every 15 min at Toulon Springs since 2007 with an accuracy of 0.5%.

Additional water samples and *in situ* measurements are performed during high-water periods and low-water periods from (i) Godet spring, an epikarstic spring from Santonian karst aquifer; (ii) Clavelie spring, representative of the saturated zone of the Cretaceous multilayered karst aquifer; and (iii) COPO spring, representative of water from deep origin. Water samples were collected semi-monthly from both Godet spring and Clavelie spring. Water samples were collected every month from COPO spring. A total of 127 samples were collected, 50 from Godet spring, 58 from Clavelie spring, and 19 from COPO spring. All springs are located within a maximul distance of a few km from Toulon Springs (Fig. 1).

Ion concentrations (Ca^{2+}, Mg^{2+}, Na^{+}, K^{+}, Cl^{-}, NO_3^{-} and SO_4^{2-}) were determined by chromatography using a Dionex ICS 1500 for the cations and using a Dionex ICS 1100 equipped (measurement accuracy 2%). Dissolved organic carbon concentrations were determined using a Shimadzu TOC 5000A TOC Analyzer (measurement accuracy 8%). Silica (SiO_2) concentrations were determined using the Strickland and

Parsons (1972) method (measurement accuracy 15%).

Fluid mineral equilibrium, e.g., saturation index with respect to calcite (SIc calcite) and CO_2 partial pressure (PCO_2), was calculated with PHREEQC software, version 3.3 (Parkhurst and Appelo, 1999).

3.2. Data processing and interpretation

A multidisciplinary approach is performed to determine the hydrogeological functioning of the Toulon karst system. This methodology combines both hydrodynamic and hydrochemical approaches, coupled with statistical approach.

3.2.1. Recession analysis

An analysis of the recession curve is usually conducted to determine the storage capacity of the system (Mangin, 1975; Bonacci, 1993; Padilla et al., 1994; Amit et al., 2002; Mudarra and Andreo, 2011; Eris and Wittenberg, 2015; Fu et al., 2016). Based on the Maillet equation (1905), Mangin (1975) concluded that an exponential equation was suitable for modeling the baseflow (Eq. 1).

$$Q(t) = Q_{R0} * e^{\alpha t} \quad (1)$$

where Q_{R0} is the initial baseflow rate and α is the baseflow recession coefficient. Although Maillet (1905) developed Eq. (1) from catchments with aquifers consisting of granulated media, it has been very widely used for karst media, i.e., non-homogeneous and anisotropic media with fissures. Numerous authors have used Eq. (1) to describe the discharge hydrograph of a karst aquifer and to identify its transportation and storage characteristics (Drogue, 1972; Atkinson, 1997; Karanjac and Altug, 1980; Bonacci, 1993; Bonacci and Jelin, 1988; Korkmaz, 1990; Soulios, 1991).

According to Mangin (1975), Bonacci (1993), Amit et al. (2002), Fu et al. (2016), baseflow recession coefficients are mostly between $10^{-1}\,day^{-1}$ and $10^{-3}\,day^{-1}$. However, El-Hakim and Bakalowicz (2007) studied some karst springs with baseflow recession coefficients of $10^{-4}\,day^{-1}$ in karst systems in the Middle East (Lebanon). In France, Touvre Springs (Charente) also exhibited a coefficient of $10^{-4}\,day^{-1}$ (Rouiller, 1987).

Recession coefficients describe the discharge of the saturated zone. Usually, a low recession coefficient implies a large saturated zone with high storage capacity. However, it could also imply baseflow support by external items from the considered karst system. It could be swallow holes situated in rivers (Touvre Springs, Chartreux spring) or supply by another aquifer.

Integrating the recession analysis over time provides the dynamic volume (Eq. 2), that is water available through the drainage from the saturated zone (Tallaksen, 1995; Amit et al., 2002; Farlin and Maloszewski, 2013).

$$V_{dyn} = \frac{Q_{R0}}{\alpha} \quad (2)$$

where V_{dyn} is the dynamic volume.

3.2.2. Time-series analysis

Univariate (auto-correlation function, ACF) and bivariate (cross-correlation function, CCF) analyses are widely used in time series analysis. These analyses could characterize the temporal structure of the hydrologic signal under linear-stationary hypotheses (Mangin, 1984; Padilla and Pulido-Bosch, 1995; Larocque et al., 1998; Labat et al., 2000; Panagopoulos and Lambrakis, 2006). The ACF examines how a value depends on the preceding values over a period of time. The graphical representation of this function is called correlogram. The slope of the correlogram characterizes the response of the system to an event. The larger the slope is, the more the karst system has a typical karstic functioning. In contrast, the lower the slope is, the less the karst system has inertial hydrodynamic responses. Usually, the length of the influence of an event is given by the memory effect, which is, according to Mangin (1984), the lag time when the ACF reaches the value of 0.2.

CCF is used to determine the relationship between two variables X and Y. Usually, these two variables have an input–output relationship, as for rainfall-discharge. This analysis gives the impulse response caused by an input signal, considered as random. Some authors have used CCF to determine the relationship between other variables, as for rainfall, electrical conductivity, turbidity, and water temperature (Larocque et al., 1998; Bouchaou et al., 2002; Amraoui et al., 2003; Genthon et al., 2005; Massei et al., 2006). The CCF is represented by a cross-correlogram, which has a positive part and a negative part. A peak in the positive part means that there is a causal relationship between the input and output time series. A peak in the negative part means that the output signal is anti-correlated with the input signal. The maximum amplitude and the lag value of the CCF provide information about delay, which indicates the time of the pressure pulse transfer into the aquifer. Shorter delay times mean faster aquifer transfer.

When rainfall is considered as input and discharge as output, correlogram, memory effect and delay time can be use to describe the karstification degree and the response of the aquifer (Covington et al., 2009; Lo Russo et al., 2014; Mayaud et al., 2014; Fu et al., 2016).

3.2.3. Classification of karst systems

The baseflow recession coefficient and the associated dynamic volume generally lead to the addition of a karst system into the classification of karst systems proposed by Mangin (1975) and modified by El-Hakim and Bakalowicz (2007). Mangin (1975) considers two indices: (i) **k**, the regulation power, defining the extent of the saturated zone of the karst system, and (ii) **i**, the infiltration delay, characterizing the infiltration conditions. The **k** parameter is the ratio between the maximum dynamic volume observed during a long-term time series and the average annual transit volume. The **i** parameter corresponds to the value of the homographic function, y (Eq. 3) at t = 2:

$$y = \frac{(1-\eta t)}{(1+\varepsilon t)} \quad (3)$$

ith the η infiltration velocity in day^{-1}, and ε the flow heterogeneity in day^{-1}.

Mangin (1975) and El-Hakim and Bakalowicz (2007) defined five domains within the space defined by **i** and **k**. Domains have been defined after calculations were performed on well-known karst systems.

3.2.4. Principal component analysis

Principal component analysis (PCA) shows the relations and correlations between variables. It is based on sample variations of variables. Variations is represented in a factorial plane composed by two factor axes. PCA is performed with standardized data, i.e., data subtracted from their average and divided by their standard deviations. Coordinates of variables in this plane range from −1 to 1 on the x-axis and on the y-axis. The more a variable is projected near the correlation circle, the more it is emphasized in the PCA. When two (or more) variables are located in the same area of this factor plane, they are positively correlated. Conversely, when two (or more) are located on opposite sides of the factor plane, they are negatively correlated.

Principal component analysis is used to identify clusters of samples that are inclined towards specific variables. PCA is usually used to describe waters of karst systems (Fournier et al., 2007; Mudarra and Andreo, 2011; Mudarra et al., 2011; Dassi, 2011; Bicalho et al., 2012; Minvielle et al., 2015).

4. Results

4.1. Hydrograph analysis

From 2007 to 2017, hydrodynamic data (rainfall and discharge) were recorded (Fig. 2). Discharge data were obtained at the outlet of the karst system. Rainfall data were obtained at rainfall stations located

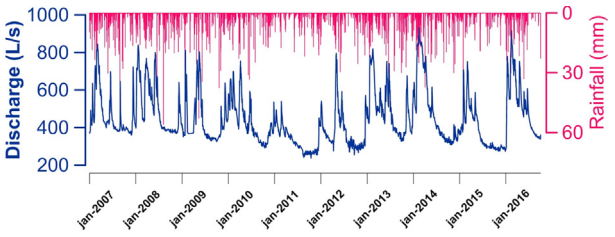

Fig. 2. Temporal evolution of daily discharge from Toulon Springs with respect to rainfall events from January 2007 to October 2016.

Table 1
Characteristics of recessions from Toulon karst system from 2007 to 2016.

Recession period	Parameters of the Maillet's function			
	Q_{R0}	t_i	α	V_{dyn}
	($L.s^{-1}$)	(day)	(10^{-4} day^{-1})	(10^6 m^3)
09/09/2007–03/12/2007	404	94	7.9	44.2
24/07/2008–24/11/2008	394	123	4.4	77.4
17/06/2009–25/09/2009	372	100	9	35.7
08/08/2012–01/12/2012	305	115	4.4	59.9
30/07/2013–01/11/2013	398	94	8	43
07/09/2014–13/11/2014	324	67	9.4	29.8
30/06/2015–01/01/2016	313	185	4.4	61.5
19/06/2016–16/11/2016	365	150	4.3	67.8

on the basin (Fig. 1). Toulon Springs have a mean annual daily discharge of 450 $L.s^{-1}$, with a minimum discharge of approximately 230 $L.s^{-1}$ (16/10/2011) and a maximum discharge of approximately 940 $L.s^{-1}$ (16/02/2014).

Seven recession curves from 2007 to 2016 were considered. The fitting procedure described previously was applied to the hydrographs of Toulon Springs (Fig. 2) to find the initial discharge baseflow (Q_{R0}), the duration of the recession (t_i), the baseflow recession coefficient (α) and the associated dynamic volume (V_{dyn}) (Table 1). The average baseflow recession coefficient and the average dynamic volume for 7 cycles are 7.10^{-4} day^{-1} and 50.2 million m^3, respectively.

Climate situations differ from one year to the next. A wet year implies a greater baseflow discharge than during a dry year. Despite these dissimilarities, calculated recession coefficients are always of the same order of magnitude (10^{-4} day^{-1}). The α coefficient is the baseflow coefficient from the aquifer when rainfall does not supply discharge at the outlet of the karst system. It is similar to the discharge of the saturated zone. This is an intrinsic characteristic of the aquifer.

The hydrological year 2014–2015, which was dry, with an annual precipitation of 612.2 mm, is a good example to study the Toulon Springs recession (Fig. 3). After a wet winter, which generated three flood events, the summer was dry and did not generate any flood event. The 2015 recession was the longest recession recorded in ten years. The recession period covered from 30/06/2015 to 01/01/2016. During this period, the baseflow recession coefficient was assessed to be 4.40×10^{-4} day^{-1}, which is close to the average. This parameter is considered a low value for a karst spring, and imply a poor drainage efficiency of the saturated zone.

On the catchment area of Toulon Springs, a baseflow support from the Beauronne river can be suspected. However, as the river is dry during the baseflow regime at Toulon Springs, this support may be negligible.

Dynamic volumes calculated from the baseflow recession coefficients are between 29.8 million m^3 and 77.4 million m^3. This result is high compared to the hydrogeological basin of the Toulon karst system (approximately 100 km^2). For comparison, Fontaine de Vaucluse karst system in France has a calculated dynamic volume of 101 million m^3 for a hydrogeological basin of 1115 km^2 (Mangin,1975).

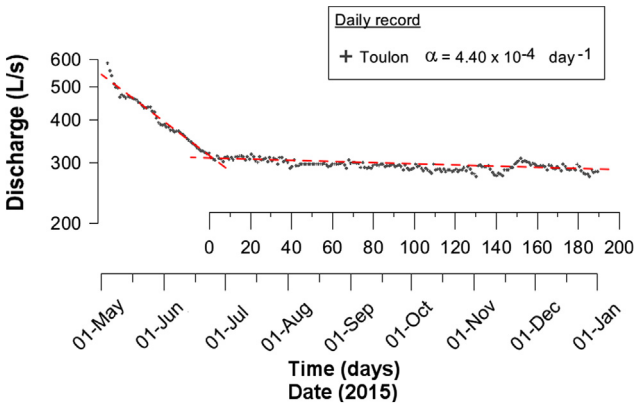

Fig. 3. Analysis of the recession curve corresponding to the hydrological year 2014–2015. Red line is the main trend of discharge evolution from May 2014 to January 2015. (For interpretation of the references to colour in this figure legend, the reader is referred to the web version of this article.)

These results provide information about the high storage capacity of the Toulon karst system and imply a large water quantity is available in the saturated zone of the karst aquifer. The complex geological situation could imply connections between several aquifers, leading to a steady discharge during low-water periods.

4.2. Auto- and cross-correlation functions

Auto-correlation functions (ACFs) and cross-correlation functions (CCFs) were performed on daily discharge measured at Toulon Springs between July 2005 and October 2016.

The ACF illustrates a memory effect of 77 days (Fig. 4A) and confirms the poor drainage efficiency of Toulon Springs, which are emptied over a long period of time. Similar results are found in bigger karst systems. For comparison, Fontaine des Chartreux karst system in France (250 km^2) and Fontaine de Vaucluse karst system (1115 km^2) have memory effects of 71 days and 75 days, respectively, according to Moussu (2011). However, smaller karst systems have a similar memory effect. For example, El Torcal karst system in Spain (28 km^2) has a memory effect of 70 days (Padilla and Pulido-Bosch, 1995).

The CCF between rainfall and discharge (Fig. 4B) provides additional information on the functioning of the Toulon karst system. In this work, all data available (rainfall and discharge) since January 2007 are used. Since rainfall can be considered as random, the results show an average impulse response of 5 days of lag time after a rainfall event, with an intensity value of 0.22 (Fig. 4B). Usually, the higher this value is, the more the karst system has the ability to transfer rainfall. To the contrary, a low value illustrates the ability of the system to filter rainfall.

The result for the bivariate analysis for Toulon Springs is in agreement with those found by a previous study, where the lag time is between hours (Bailly-Comte et al., 2008; Covington et al., 2009; Mayaud et al., 2014) and days (Padilla and Pulido-Bosch, 1995; Larocque et al., 1998; Panagopoulos and Lambrakis, 2006). The CCF shows that a quickflow component is present (average response of 5 days after a rainfall event). However, a large part of the input signal is filtered through the karst system (CCF of 0.22). The low slope from 25 to 70 days may confirm the predominance of the baseflow component at the outlet of the karst system. This value (70 days) is a measure of the length of the impulse response of the system. According to the recession analysis, it means that the CCF shows predominantly the hydrologic response of the system being influenced by fast infiltration (before 5 days).

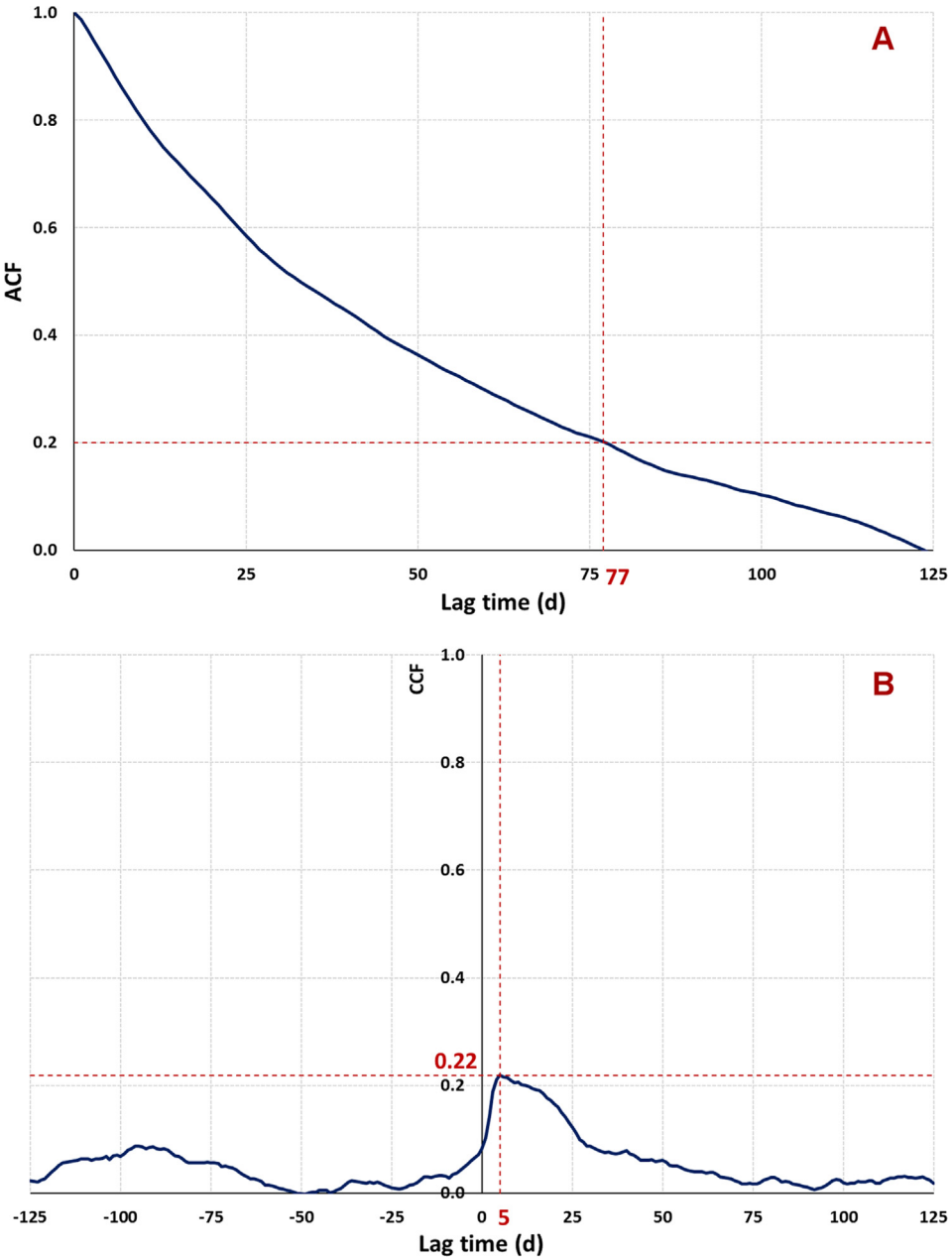

Fig. 4. (A): Auto-correlation of Toulon Springs daily discharge from 2007 to 2017. (B): cross-correlation function of the Toulon Springs daily discharge and daily rainfall from 2007 to 2017.

4.3. Chemograph analysis

From February 2014 to October 2017, hydrodynamic and hydrochemical data were obtained in different water conditions (recharge, recession, depletion). Table 2 summarizes the main hydrochemical data of Toulon Springs, Godet spring, Clavelie spring and COPO spring (Fig. 1). Fig. 5 illustrates the temporal evolution of discharge and hydrochemical parameters from Toulon Springs

Analysis of hydrochemical parameters from Toulon Springs distinguish two main water types: (i) typical low-water period hydrochemical signature, with good water quality, and (ii) high-water period hydrochemical signature, with indices of surface contamination which illustrate quick responses of the karst system.

Water from low-water periods, usually measured from summer to autumn, is described by warmer water (14.40 °C) compared to regional springs (12.5 °C) as described by Peyraube et al. (2012), Peyraube et al. (2013), Houillon et al. (2017); and with Mg concentration ($\sim$12.00 mg.L^{-1}) and O_2 concentration ($\sim$4.00 mg.L^{-1}). Electrical conductivity (EC) and HCO_3 concentration are stable ($\sim$590 µS.cm^{-1} and $\sim$350 mg.L^{-1}). Associated with low discharge, at the outlet of the karst system, water quality is better. Turbidity is below the French standard for potability ($\sim$0.20 NTU). NO_3^- concentration and D.O.C. concentration are also lower than during high-water periods ($\sim$10 mg.L^{-1} and $\sim$0.20 mg.L^{-1}). During the low-water periods, water is in equilibrium with calcite (SIc $\sim$ 0.00) and has PCO_2 values lower than during high-water periods ($\sim$2.50%). Despite these similarities observed every year, the climate situation forces different natural responses at Toulon springs.

Water from high-water periods is usually measured during the winter and spring. During this period, high rainfall intensity implies quick hydrochemical variations at Toulon Springs, associated with aquifer recharge. High-water periods during 2015, 2016 and 2017 are contrasted. Winters in 2015 and 2017 winters experienced little rain, and discharge responses were low, with only a few floods of low

Table 2
Statistical parameters of the waters samples analyzed from Toulon Springs, Godet spring, Clavelie spring and COPO spring during the study period from February 2014 to October 2017. (n) number of samples, (σ) standard deviation, (CV) coefficient of variation.

		Q	pH	T	EC	O2	Ca	Mg	HCO3	SO4	NO3	SIc	PCO2	DOC	Turbidity
		(L/s)	(pH unit)	(°C)	(µS/cm)	(mg/L)	(mg/L)	(mg/L)	(mg/L)	(mg/L)	(mg/L)		(%)	(mg/L)	(NTU)
Toulon Springs	n	1465	759	759	1465	759	187	187	187	187	651	187	187	651	1465
	Mean	459.5	7.0	13.8	585	5.2	108.7	7.3	334.0	8.9	12.7	−0.1	2.9	0.9	1.5
	Min	273.5	6.9	12.8	533	3.7	101.8	3.1	290.4	7.4	10.0	−0.2	2.2	0.2	0.1
	Max	932.5	7.1	14.4	608	7.6	116.3	12.8	356.1	10.6	19.7	0.0	3.9	3.4	13.7
	σ	157.6	0.0	0.4	11.4	1.0	3.4	2.7	14.2	0.7	1.7	0.1	0.3	0.7	1.8
	CV (%)	34.3	0.6	3.2	1.9	19.2	3.1	37.5	4.2	7.7	13.5	58.4	10.6	83.0	122.4
Godet spring	n		50	50	50	50	50	50	50	50	50	50	50	50	32
	Mean		6.80	12.3	559	7.9	111.8	2.4	324.1	8.1	9.8	−0.3	4.0	1.2	1.0
	Min		6.7	11.9	367	7.4	65.7	1.9	195.4	6.8	5.8	−0.8	2.8	0.4	0.0
	Max		6.9	12.5	629	8.4	131.4	3.0	374.5	10.8	14.3	−0.1	4.9	3.8	6.2
	σ		0.1	0.1	53.6	0.2	14.1	0.3	34.9	1.1	2.4	0.1	0.6	0.8	1.5
	CV (%)		0.8	1.1	9.6	3.1	12.7	11.8	10.8	13.7	24.4	46.8	14.0	67.3	155.3
Clavelie spring	n		58	58	58	58	58	58	58	58	58	58	58	58	32
	Mean		6.9	13.7	629	4.4	122.5	3.8	359.8	8.7	16.9	−0.1	3.7	1.7	1.6
	Min		6.8	12.9	552	2.8	112.0	1.8	293.9	7.3	10.1	−0.2	2.8	0.7	0.3
	Max		7.0	14.2	660	7.2	130.7	5.9	379.8	12.1	28.9	0.0	4.6	4.1	10.4
	σ		0.0	0.4	22.7	1.3	4.3	1.1	18.5	1.0	4.9	0.0	0.4	0.9	2.1
	CV (%)		0.5	2.7	3.6	29.0	3.5	30.1	5.1	11.5	29.0	52.1	9.8	52.3	136.1
COPO spring	n		19	19	19	19	19	19	19	19	19	19	19	19	13
	Mean		7.1	20.4	551	1.6	81.7	22.3	329.7	9.4	7.3	0.0	2.2	0.6	0.1
	Min		7.0	20.2	530	1.4	72.3	21.5	320.9	8.3	4.9	−0.1	2.0	0.3	0.0
	Max		7.2	21.2	568	1.9	87.0	23.2	334.7	11.7	9.0	0.1	2.7	1.0	0.1
	σ		0.0	0.2	8.7	0.2	2.9	0.6	3.9	1.2	1.1	0.0	0.2	0.2	0.0
	CV (%)		0.6	1.1	1.6	9.9	3.6	2.5	1.2	12.9	15.0	−133.7	10.0	40.0	85.0

magnitude. In contrast, after a low-water period of six months, the 2016 winter was very rainy (~582 mm from January to June).

A rainy situation exhibits the occurrence of several long flood events of high magnitude. Hydrochemical natural responses are quite similar from one hydrological cycle to another. Natural tracers evolve, associated with discharge:

1) Pressure transfer propagating into the karst system enables an increase of turbidity values and a mobilization of more mineralized waters stored in the saturated zone. This arrival of water is characterized by an increase in electrical conductivity (~605 µS.cm^{-1}).
2) Then, mass transfer implies a decrease in water mineralization, illustrated by a decrease in electrical conductivity (~520 µS.cm^{-1}) and a decrease in HCO_3 concentrations (~290.00 mg.L^{-1}) and Mg concentrations (~3.00 mg.L^{-1}). The decrease in water temperature (~12.80 °C) and increase in O_2 concentration (~7.5 mg.L^{-1}) and D.O.C. concentration (~2.50 g.L^{-1}) characterize a quick infiltration from surficial waters during recharge events. Water flowing at Toulon Springs is under-saturated with respect to calcite (~ −0.25) and has the greatest PCO_2 concentration (~3.8%).

4.4. Principal component analysis

A principal component analysis (PCA) was conducted using data from Toulon Springs, coupled to other waters types observed in the study area: (i) waters from COPO spring, representative of water from the Jurassic; (ii) waters from Clavelie spring, representative of the Cretaceous saturated zone; and (iii) waters from Godet spring, representative of Cretaceous superficial aquifers water. The PCA is based on 298 samples (171 from Toulon Springs, 19 from COPO spring, 58 from Clavelie spring, and 50 from Godet spring) collected from February 2014 to October 2017 and 12 variables (T, pH, O_2, EC, Ca, Mg, HCO_3, NO_3, DOC, SiO_2, SIc, and PCO_2). The first factor plane (F1-F2) explains 75.52% of the total variance. The results of the PCA are presented through the variable space (Fig. 6).

The first axis (F1) is explained by T, pH, SIc, and Mg in its positive part and Ca, SiO_2, PCO_2 and O_2 in its negative part. Water origins can be qualified with the F1-axis: “Jurassic waters” in its positive part and “Cretaceous waters” in its negative part. Toward the positive part, waters tend to have an increasing proportion of deep waters from the Jurassic aquifer. The second axis (F2) is explained by EC and HCO_3 in its positive part and O_2 and D.O.C. in its negative part. It represents “Cretaceous saturated zone waters” in its positive part and “Infiltration waters” in its negative part.

Waters from Godet spring are scattered between two poles (Fig. 6): (i) “New recharge water” during high-water periods and (ii) “Cretaceous saturated zone waters” during low-water periods. Godet spring can be seen as a good example of a karst spring fed by a single aquifer.

Waters from Clavelie spring are mainly located in the positive part of the F2-axis and can be qualified as “Cretaceous saturated zone waters”. However, during winter flood events, samples can move towards the negative part of the F2-axis and can be associated with a majority of “New recharge water” (Fig. 6).

Waters from COPO spring are only located in the positive part of the F1-axis and constitute the “Jurassic waters” pole (Fig. 6). These waters show few hydrochemical variations. It is mainly characterized by warm waters (~20.40 °C), with high magnesium concentration (~22.3 mg.L^{-1}) and low dissolved oxygen concentration (~1.60 mg.L^{-1}).

Waters from Toulon Springs are expanded along the 3 main poles represented in this PCA (Fig. 6):

1) During high-water periods, “New recharge water” explains the majority of waters flowing to Toulon Springs.
2) At the beginning of the recession, waters evolve towards the positive part of the F2-axis. The proportion of “Infiltration waters” decreases, and the proportion of “Cretaceous saturated zone waters” increases, associated with the decrease in discharge.
3) Finally, during low-water periods, waters flowing at Toulon Springs evolve towards the positive part of the F1-axis, leading to a mixture of “Cretaceous saturated zone waters” with “Jurassic waters”.

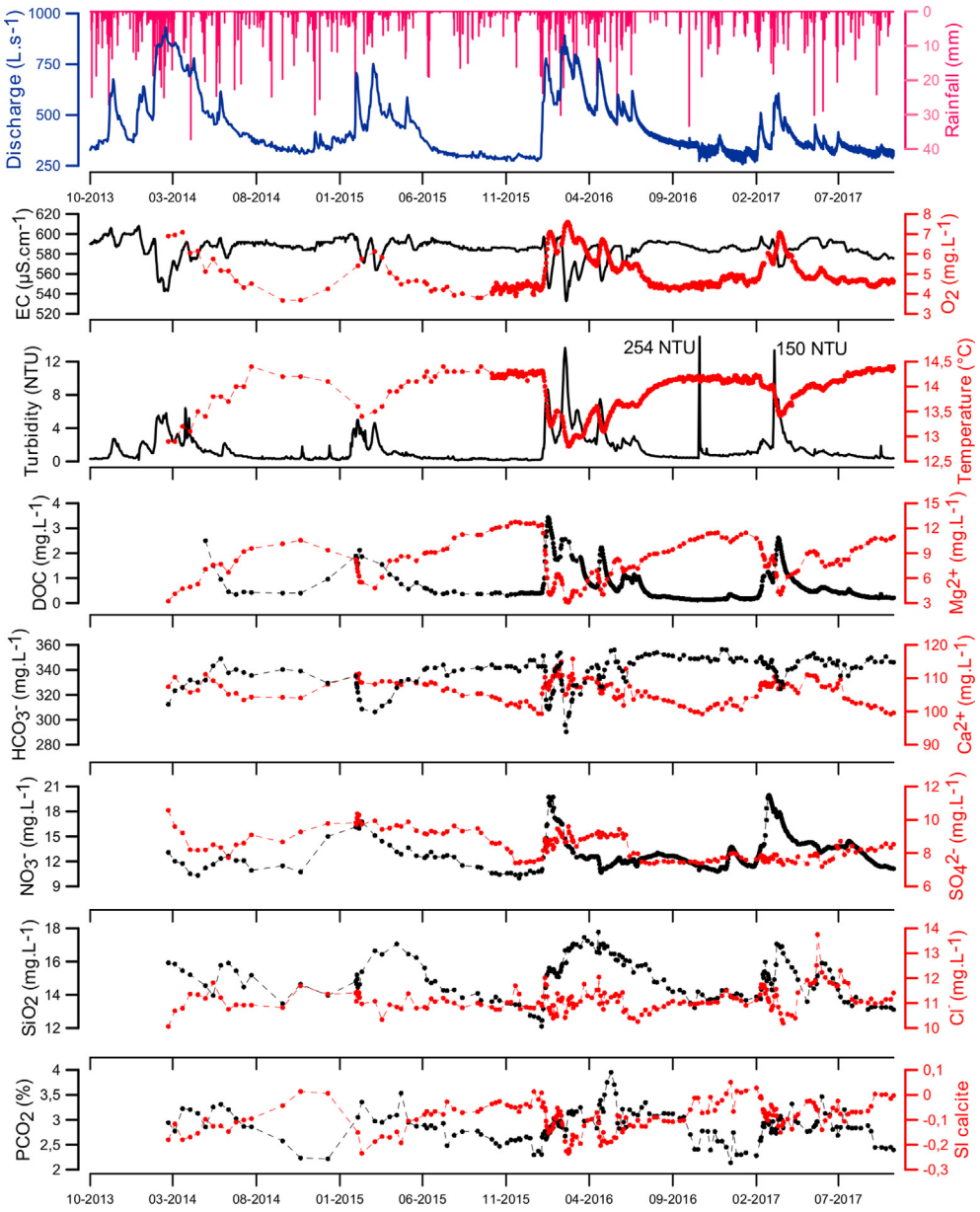

Fig. 5. Temporal evolution of discharge and hydrochemical parameters from Toulon Springs with respect to rainfall events from October 2013 to October 2017.

5. Discussion

5.1. Classification of karst systems

Calculated parameters (**i** and **k**) situate Toulon Springs into the classification of karst systems. According to Fig. 7, Toulon Springs are located in Domain 5 added by El-Hakim and Bakalowicz (2007).

Before this study, the Touvre karst system was the only French karst system, which was also located in domain 5. Despite their proximity in the classification, Touvre Springs and Toulon Springs do not exhibit the same functioning. Touvre Springs are fed by swallow holes (50%) located in a river, implying steady baseflow discharge during low-water periods (Larocque, 1997). Consequently, the calculated dynamic volume at Touvre Springs does not represent the stock of water available to the saturated zone of the aquifer. In contrast, the calculated dynamic volume at Toulon Springs represents the water available to the saturated zone of the aquifer. During low-water periods, this stock supports the discharge at the outlet of the karst system, implying a steady discharge.

El Torcal karst system cannot be part of this classification because the **i** parameter cannot be estimated.

5.2. New recharge water and vulnerability of the Toulon karst system

From a contamination point of view, nitrate is a relevant parameter. Nitrate responses in karst systems can have various scenarios: (i) mobilized nitrate concentrations (Pronk et al., 2009), (ii) diluted nitrate concentrations (Mahler et al., 2008), (iii) a combination of mobilized and diluted nitrate concentrations during a single flood event (Rowden et al., 2001), (iv) mobilized and diluted nitrate concentrations during multiple events (Stueber and Criss, 2005). Predominance of mobilization or dilution of nitrate concentration during storm events depends highly on the availability of nitrate accumulates in soil and the unsaturated zone. Rainfall events have an influence on the intensity and time lag of nitrate concentration changes (Huebsch et al., 2014).

In the Toulon karst system, diffuse NO_3^- contamination from the surface exhibits NO_3^- concentrations in the saturated zone between 11 $mg.L^{-1}$ and 12 $mg.L^{-1}$. These same concentrations are found at

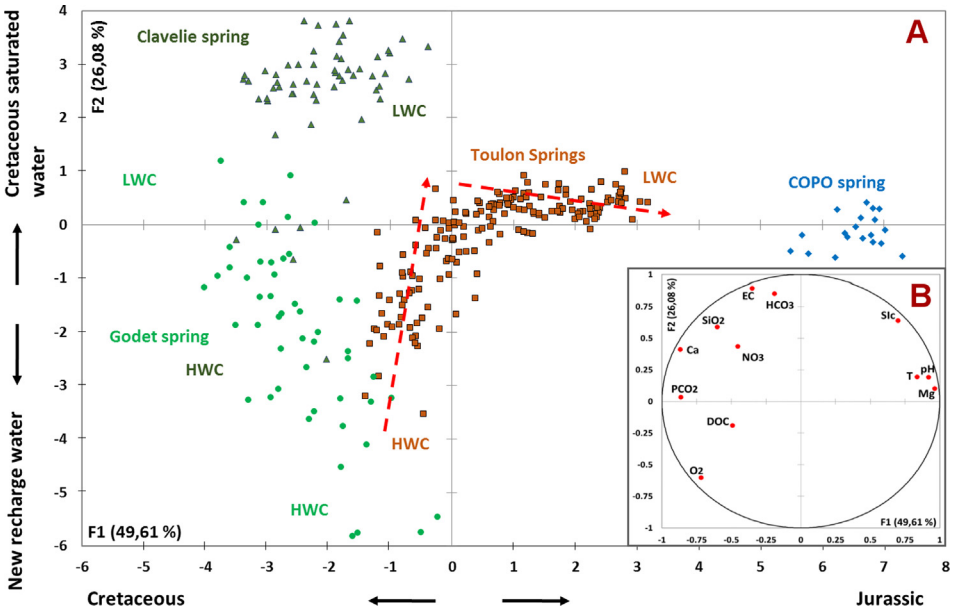

Fig. 6. (A) Variable space in the first factor plane based on water from Toulon Springs, Clavelie spring, COPO spring, and Godet spring. (B) Sample space in the first factorial plane based on the same springs. LWP: Low-water periods, HWP: high-water period. Red line is the main trend of Toulon water evolution from LWP to HWP. (For interpretation of the references to colour in this figure legend, the reader is referred to the web version of this article.)

Toulon Springs when the system is not influenced by rainfall. During recharge events, the first flood event leads to an increase of NO_3^- concentrations (16.58 mg.L^{-1} on 06/02/2015 and 19.3 mg.L^{-1} on 18/01/2016), associated with an increase in D.O.C. concentrations. The increase in concentrations results in the mobilization of NO_3^- storage in soil and the unsaturated zone of the aquifer during low-water periods. Then, associated with the next flood events, NO_3^- concentrations were under the value of 12 mg.L^{-1} (10.31 mg.L^{-1} on 16/04/2014 and 10.51 mg.L^{-1} on 23/04/2016), indicating that the main stock of NO_3^- storage in the soil and the unsaturated zone of the aquifer was moved to the outlet of the karst system during the previous flood event. The decrease in NO_3^- concentrations is still associated with an increase in D.O.C. concentration (3.22 mg.L^{-1} on 16/04/2014 and 2.26 mg.L^{-1} on 23/04/2016), indicating that dilution water has the same of origin.

5.3. Magnesium–dissolved oxygen relationships

High magnesium concentrations observed during low-water periods are uncommon for a water resource associated with the Turonian aquifer in Dordogne. Recently, regional studies (Peyraube et al., 2012; Houillon, 2016) show low magnesium concentrations in upper Cretaceous aquifers (less than 5 mg.L^{-1} as a result of the absence of dolomite). The question of the origin of magnesium concentrations is one of the main objectives associated with the hydrogeological functioning of the Toulon karst system. High values of magnesium concentration are only observed in confined Jurassic aquifers (more than 20 mg.L^{-1} as a result of the presence of magnesium-calcite). Local complex hydrogeological situations associated with possible relationships between upper Jurassic and upper Cretaceous aquifers make it difficult to understand the origin of magnesium in Toulon Springs.

Dissolved oxygen is a relevant parameter for the Toulon karst system. Usually, in karst aquifers, good connection with the atmosphere

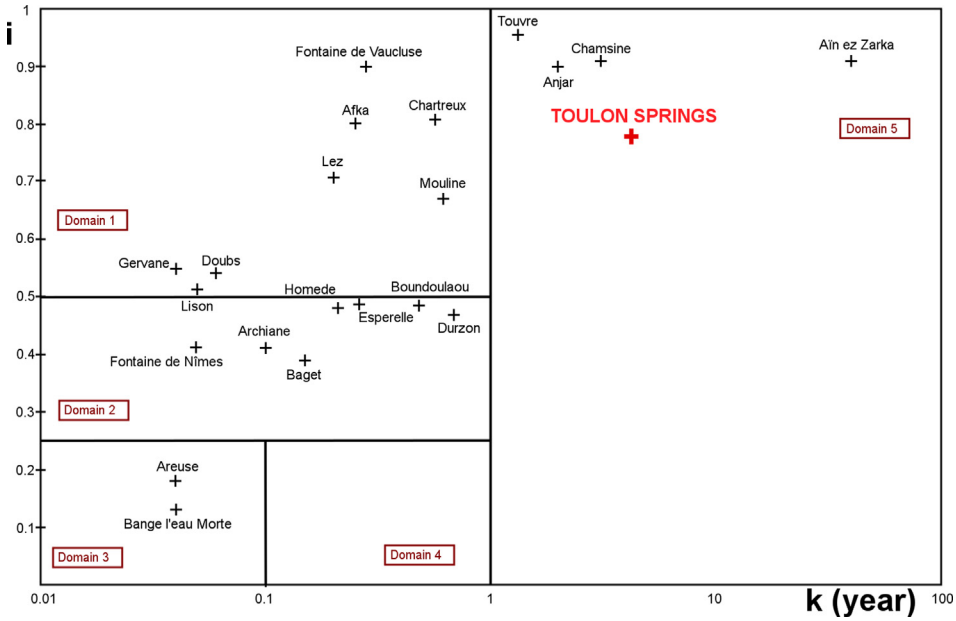

Fig. 7. Classification of karst systems based on indices from the recession analysis (adapted from El-Hakim and Bakalowicz, 2007; Moussu, 2011).

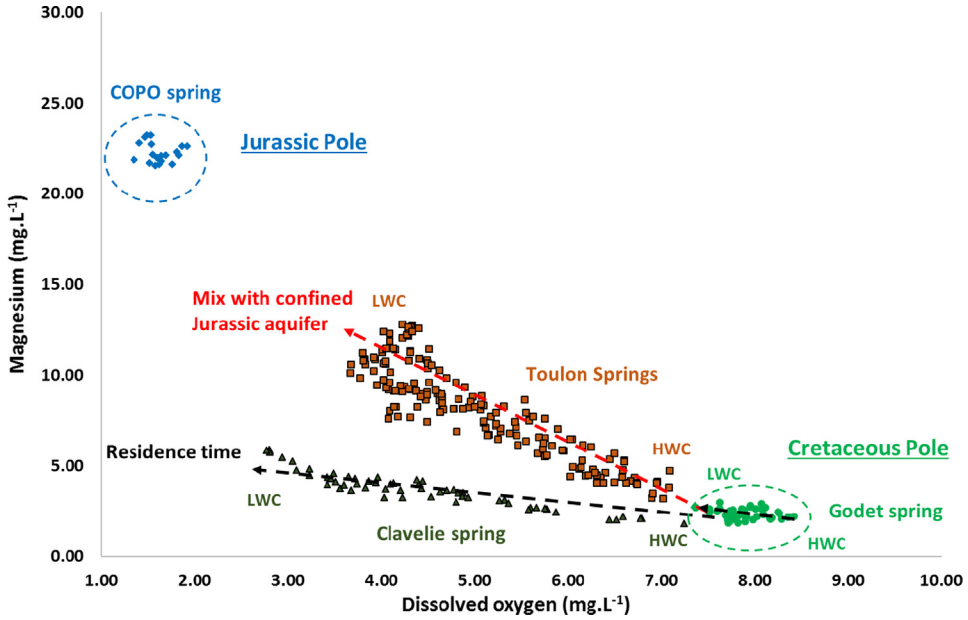

Fig. 8. Magnesium vs dissolved oxygen diagram for all of the Toulon karst system springs. COPO appears as a pole for Jurassic water. LWP: low-water period, HWP: high-water period.

implies oxic waters at the outlet of the karst system (Perrin et al., 2007; Mahler et al., 2011; Musgrove et al., 2011). Deep water mobilization could be responsible for low O_2 concentrations observed at Toulon Springs during low-water periods. This phenomenon has already been demonstrated at Barton springs (Estafanía et al., 2011; Mahler and Bourgeais, 2013).

The comparison of O_2 concentration and magnesium concentration (Fig. 8) from springs presented in this current work shows that O_2 alone is not a relevant parameter to the mobilization of waters from the Jurassic confined aquifer. Clavelie spring, representative of an upper Cretaceous saturated zone, has similar O_2 concentrations as Toulon Springs (Table 2). However, magnesium concentrations are lower (5.88 on 08/12/2015). During high-water periods, Clavelie and Toulon waters are very close on this diagram, confirming the similar origin of their waters, as noticed in the PCA (Fig. 6). During low-water periods, the O_2 vs Mg diagram (Fig. 8) identifies two straight lines: (i) the first one increasing from high water of Toulon Springs to COPO spring waters, indicating the mixture with a Jurassic confined aquifer, and (ii) the second one increasing toward the low waters of Clavelie spring, illustrating the residence time of the water in the aquifer and the magnesium-calcite dissolution.

5.4. Toulon Springs conceptual functioning

The complex hydrogeological situation of the Toulon karst system includes two multilayered karst aquifers: (i) a fractured and karstified multilayered Cretaceous aquifer (Turonian, Coniacian, and Santonian); (ii) a Jurassic dolomitic limestone multilayered karst aquifer (Kimmeridgian, Oxfordian, Bathonian, and Bajocian). The approach used in this work aims to evaluate the relationships between these aquifers.

The first step is to identify the inertial behavior of Toulon Springs during low-water periods, associated with a high dynamic volume (Recession analysis, ACF). These characteristics are not usual for a French karst system, illustrating the importance of this karst system from a drinking water point of view. A part of this work was to evaluate the quick flow component during a recharge event (CCF). Hydrodynamic tools were used to conduct the evaluation of dual behavior between high-water periods and low-water periods.

The second step was to exhibit the natural hydrochemical characteristics of water. Two main water types were identified: (i) a first one during low-water periods, associated with a deep origin with good water quality (Fig. 9B), and (ii) a second one during high-water periods, associated with quick infiltration from surficial waters during recharge events (Fig. 9A). The comparison of different water types observed in the study area (PCA) leads to the identification of the main components that fed Toulon Springs (Fig. 9): (i) confined Jurassic karst aquifer and (ii) unconfined Cretaceous karst aquifer. The contribution rates between these two end-members are different, according to the hydrological conditions. During low-water periods, Jurassic aquifer contribution is more important than during high-water periods In contrast, during high-water periods, the upper Cretaceous aquifer mainly participates to the flow of Toulon Springs.

The complex geological situation of the edge of the sedimentary basin involves difficulties in the recharge evaluation of deep aquifers. Over the study area, Jurassic confined karst aquifer and Cretaceous karst aquifer are supposedly separated by Cenomanian marls (Fig. 1). Upstream of Toulon Springs, the recharge of the Jurassic aquifer can operate in confined or unconfined parts. In unconfined parts, recharge is possible if: (i) Cenomanian becomes sandy and (ii) the Jurassic hydraulic head is below the Cretaceous one. Due to the lack of data about lithological facies variations or piezometric level, the hypothesis of recharge cannot be proven yet.

6. Conclusion

The first objective was to assess the water quantity available into the Toulon karst system using natural hydrodynamic responses. The second one was to assess the water quality using natural hydrochemical responses. The third one was to combine these tools to evaluate the functioning of a typical example of a complex karst system drained by two multilayered karst aquifers located on the northern edge of a sedimentary basin, proposing a conceptual model of functioning. Observations coupled to knowledge of the complex hydrogeological situation suggest that Toulon Springs flow is fed by a mixing of two aquifers: (i) the Jurassic confined karst aquifer (Oxfordian, Kimmeridgian, Bathonian, and Bajocian), which is responsible for low-water period support and related to dolomitic hydrochemical characteristics, and (ii) the upper Cretaceous unconfined aquifer (Turonian, Coniacian, and Santonian), which is responsible for quick

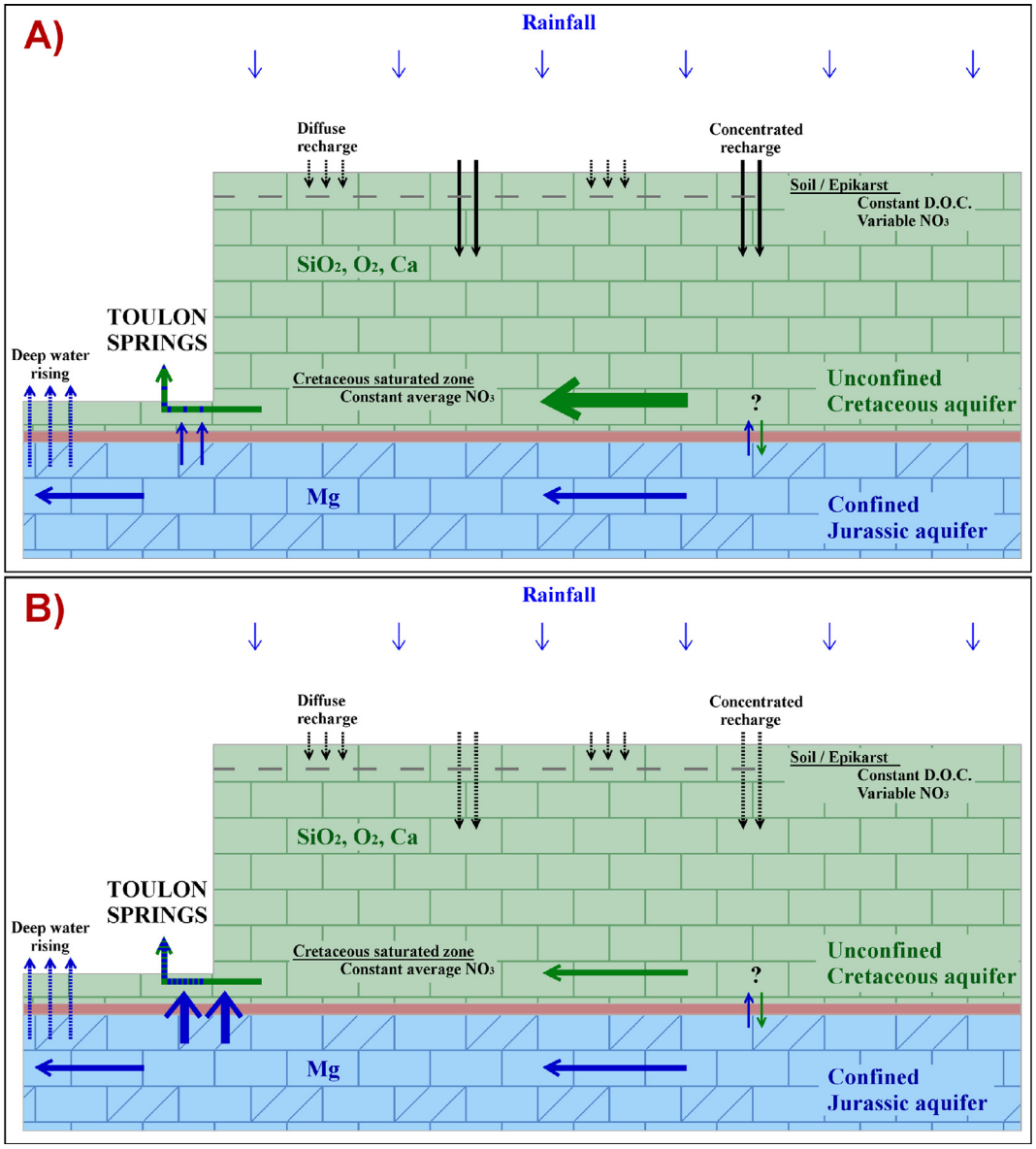

Fig. 9. Conceptual model of the functioning of Toulon karst system. A) High-water period. B) Low-water periods.

hydrodynamic and hydrochemical variations observed at Toulon Springs.

We suggest discussions about the common use of magnesium concentrations and dissolved oxygen concentrations to differentiate (i) the mixture between two aquifers (as a result of the presence of magnesium-calcite) and (ii) an increase in the residence time of the water (as a result of the absence of dolomite). The O_2 vs Mg diagram is an innovative tool to use in complex hydrogeological situations with complex relationships between aquifers (dolomitic and limestone aquifers).

This methodology, based on both hydrodynamic and hydrochemical natural responses, is an efficient tool to characterize the functioning of a complex multilayered karst system located on the edge of a sedimentary basin. The main advantage is the easy way of implementing the method, leading to an easy method of comparison between karst systems.

Acknowledgements

This work was supported by the Région Aquitaine, the city of Périgueux, Suez, the Conseil Général de la Dordogne, and the Adour-Garonne Water Agency. The authors thank Suez's agents for the technical assistance and the field knowledge they contributed. The authors thank Valentine Busquet and Jonathan Sabidussi for their help and support both in the field and laboratory. The authors finally thank the CER SNCF for the free access to COPO spring.

This work benefited from fruitful discussion within the KARST observatory network (SNO KARST) initiative from the INSU/CNRS. SNO KARST aims to strengthen knowledge sharing and to promote cross-disciplinary research on karst systems at the national scale.

References

Amit, H., Lyakhovsky, V., Katz, A., Starinsky, A., Burg, A., 2002. Interpretation of spring recession curves. Ground Water 40 (5), 543–551.

Amraoui, F., Razack, M., Bouchaou, L., 2003. – Turbidity dynamics in karstic systems. Exemple of Ribaa and Bittit springs in the Middle Atlas (morocco). Hydrol. Sci. J. 48 (6), 971–984.

Atkinson, T., 1997. Carbone dioxide in the atmosphere of the unsaturated zone: an important control of groundwater hardness in limestones. J. Hydrol. 35, 111–123.

Audra, P., Gasquez, F., Rull, F., Biguot, J.-Y., Camus, H., 2015. Hypogene Sulfuric Acid Speleogenesis and rare sulfate minerals in Baume Galinière Cave (Alpes-de-Haute-Provence, France). Record of uplift, correlative cover retreat and valley dissection. Geomorphology 247, 25–34.

Bailly-Comte, V., Jourde, H., Roesch, A., Pistre, S., Batiot-Guilhe, C., 2008. Time series

analyses for karst/river interactions assessment: case of the Coulazou River (southern France). J. Hydrol. 349 (1–2), 98–114.
Bakalowicz, M., 1995. La zone d'infiltration des aquifers karstiques Méthodes d'étude. Structure et fonctionnement. Hydrogéologie 4, 3–21.
Bakalowicz, M., 2005. Karst groundwater: a challenge for new resources. Hydrogeol. J. 13, 148–160.
Batiot, C., Linan, C., Andreo, B., Emblanch, C., Carrasco, F., Blavoux, B., 2003b. Use of TOC as tracer of diffuse infiltration in a dolomitic karst system: the Nerja Cave (Adalousia, southern Spain). Geophys. Res. Lett. 30, 2179.
Batiot, C., Emblanch, C., Blavous, B., 2003a. Carbone organique total (COT) et Magnésium (Mg2+): deux traceurs complémentaires du temps de séjours dans l'aquifère karstique. CR Géosci. 335, 205–214.
Bicalho, C., Batiot-Guilhe, C., Seidel, J.L., Van Exter, S., Jourde, H., 2012. Geochemical evidence of water characteriz1ation and hydrodynamic responses in a karst aquifer. J. Hydrol. 450–451, 206–218.
Birk, S., Liedl, R., Sauter, M., 2004. Identification of a localized recharge and conduit flow by combined analysis of hydraulic and physico-chemical sopring responses (Urenbrunnen, SW-Germany). J. Hydrol. 286, 179–193.
Bonacci, O., 1993. Karst springs hydrographs as indicators of karst aquifer. Hydrogeol. J. Sci. 386 (1–4), 55–66.
Bonacci, O., Jelin, J., 1988. Identification of a karst hydrological system in the Dinaric karst (Yogoslavia). Hydrol. Sci. J. 33 (5), 483–497.
Bouchaou, L., Mangin, A., Chauve, P., 2002. Turbidity mechanism of water from a karstic spring: example of the Ain-Asserdoune spring (beni Mellal Atlas, Marocco). J. Hydrol. 265, 34–42.
Brkic, Z., Kuhta, M., Hunjak, 2018. Groundwater flow mechanism in the well-developed karst aquifer system in the western Croatia: insights from spring discharge and water isotopes. Catena 161, 14–26.
Covington, M.D., Wicks, C.M., Saar, M.O., 2009. A dimensionless number describing the effects of recharge and geometry on discharge from simple karstic aquifer. Water Resour. Res. 45 (11), W11410.
Cubaynes, R., Faure, P., Hantzpergue, P., Pélissié, T., Rey, J., 1989. Le jurassique du Quercy: unités lithostratigraphiques, stratigraphie et organisation séquentielle, évolution sédimentaire. Géol. Fr. 3, 33–62.
Dassi, L., 2011. Investigation by multivariate analysis of groundwater composition in a multilayer aquifer system from North Africa: a multi-tracer approach. Appl. Geochem. 26, 1386–1398.
Doctor, D.H., Alexander Jr., E.C., Petric, M., Kogovsek, J., Urbanc, J., Lojen, S., Stichler, W., 2006. Quantification of karst aquifer discharge components through endmember mixing analysis using natural chemistry and isotopes as tracers. Hydrogeol. J. 14, 1171–1191.
Drogue, C., 1972. Analyse statistique des hydrogrammes de décrues des sources karstiques. J. Hydrol. 16, 49–68.
El-Hakim, M., Bakalowicz, M., 2007. Significance and origin of very large regulating power of some karst aquifers in the Middle east. Implication on karst aquifer classification. J. Hydrol. 333, 329–339.
Emblanch, C., Blavoux, B., Puig, J.M., Mudry, J., 1998. Dissolved organic carbon of infiltration within the autogenic karst hydrosystem. Geophys. Res. Lett. 25, 1459–1462.
Emblanch, C., Zuppi, G.M., Mudry, J., Blavoux, B., Batiot, C., 2003. Carbon 13 of TDIC to quantify the role of the unsaturated zone: the example of the Vaucluse karst system (Southeastern France). J. Hydrol. 279 (1–4), 262–274.
Eris, E., Wittenberg, H., 2015. Estimation of baseflow and water transfer in karst catchments in Mediterranean Turkey by nonlinear recession analysis. J. Hydrol. 530, 500–507.
Estafanía Lazo-Herenda, S., Hunt, B.B., Smith, B.A., Gary, R.H., 2011. A survey of dissolved oxygen in groundwater during drought conditions. Barton Springs segment of the Edwards aquifer. Central Texas. In: World Lakes Conference. Austin, Texas.
Farlin, J., Maloszewski, P., 2013. On the use of spring baseflow recession for a more accurate parametrization of aquifer transit time distribution functions. Hydrol. Earth Sci. 17 (5), 1825–1831.
Filippini, M., Squarzoni, G., De Waele, J., Fiorucci, A., Vigna, B., Grillo, B., Riva, A., Rossetti, S., Zini, L., Casagrande, G., Stumpp, C., Gargini, A., 2018. Differentiated spring behavior under changing hydrological conditions in an alpine karst aquifer. J. Hydrol. 556, 572–584.
Ford, D., Willians, P., 2007. Karst Hydrogeology and Geomorphology, second ed. Chichester Wiley.
Fournier, M., Massei, N., Bakalowicz, M., Dussart-Baptista, L., Rodet, J., Dupont, J.P., 2007. Using turbidity dynamics and geochemical variability as a tool for understanding the behavior and vulnerability of a karst aquifer. Hydrogeol. J. 15 (4), 689–704.
Fu, T., Chen, H., Wang, K., 2016. – Structure and water storage capacity of a small karst aquifer based on stream discharge in southwest China. J. Hydrol. 534, 50–62.
Genthon, P., Bataille, A., Fromant, A., D'Hulst, D., Bourges, F., 2005. Temperature as a marker for karstic waters hydrodynamics. Inferences from 1 year recording at La Peyrére cave (Ariège; France). J. Hydrol. 311, 157–171.
Grasso, D.A., Jeannin, P.Y., Zwahlen, F., 2003. A deterministic approach to the coupled analysis of karst springs hydrographs and chemographs. J. Hydrol. 271, 65–76.
Houillon, N., 2016. la dynamique du carbone inorganique dans le continuum sol-épikarst-cavité du site de la grotte de Lascaux (Dordogne, France): apports des monitorings hydrogéochimiques et microclimatiques continus pour l'étude de l'aérologie et le développement d'une méthode de simulation des processus calco-carboniques aux paroirs. Thèse de Doctorat en sciences naturelles. Université de Bordeaux, pp. 370.
Houillon, N., Lastennet, R., Denis, A., Malaurent, P., Minvielle, S., Peyraube, N., 2017. Assessing cave internal aerology in understanding carbon dioxide (CO_2) dynamic: implications on calcite mass variation on the wall of Lascaux cave (France). Environ. Earth Sci. 76, 70.
Huebsch, M., Fenton, O., Horan, B., Hennessy, D., Richards, K.G., Jordan, P., Goldscheider, N., Butscher, C., Blum, P., 2014. Mobilisation or dilution ? Nitrate response of karst springs to high rainfall events. Hydrol. Earth Syst. Sci. 18, 4423–4435.
Husson, E., Camus, H., Lerouge, C., Lasseur, E., Coueffe, R., Cabaret, O., Pedron, N., 2016. Origin of karst on the northeast edge of the Aquitaine Basin: a multiphase and complex evolution. In: Eurokarst 2016. Neuchâtel.
Karanjac, J., Altug, A., 1980. Karstic spring recession hydrograph and water temperature analysis: oymapinar Dam Project, turkey. J. Hydrol. 45, 203–217.
Klimchouk, A., 2007. Hypogene Speleogenesis: Hydrogeological and Morphogenetic Perspective. Special Paper no. 1.. National Cave and Karst Research Institute,, Carlsbad, NM., pp. 106.
Klimchouk, A., 2012. Speleogenesis, hypogenic. In: Ecyclopedia of caves. pp. 748–765.
Korkmaz, N., 1990. The estimation of groundwater recharge from spring hydrographs. Hydrol. Sci. J. 35 (2), 209–217.
Labat, D., Abadou, R., Mangin, A., 2000. Rainfall-runoff relations for karstic springs. Part I: convolution and spectral analyses. J. Hydrol. 238 (3-4), 123–148.
Larocque, M., 1997. Intégration d'approches quantitatives de caractérisation et de simulation des aquifères calcaires fissurés – application à l'aquifère karstique de la Rochefoucald (Charentes, France). Université de Poitiers Thèse de Doctorat en sciences naturelles.
Larocque, M., Mangin, A., Razack, M., Banton, O., 1998. Contribution of correlation and spectral analyses to the regional study of a large karst aquifer (Charente, France). J. Hydrol. 205, 217–231.
Lastennet, R., 1994. Rôle de la zone non saturée dans le fonctionnement des aquifères karstiques. Approche par l'étude physico-chimique et isotopique du signal d'entrée et des exutoires du massif du Ventoux (Vaucluse). Thèse de Doctorat en sciences naturelles. Université d'Avignon et des pays de Vaucluse.
Lastennet, R., Huneau, F., Denis, A., 2004. Geochemical characterization of complex multilayer karstic systems. Springs of Périgueux, France. In: Proceedings of the international Transdisciplinary Conference on Development and Conservation of Karst Regions. Hanoi, Vietnam. pp. 132–135.
Lastennet, R., Mudry, J., 1997. Role of karstification and rainfall in the behavior of a heterogeneous karst system. Environ. Geol. 32 (2), 114–123.
Lo Russo, S., Amanzio, G., Ghione, R., De Maio, M., 2014. Recession hydrographs and time series analysis of springs monitoring data: application on porous and shallow aquifers in mountain areas (Aosta Valley). Environ. Earth Sci. 73 (11), 7415–7434.
Lorette, G., Lastennet, R., Peyraube, N., Denis, A., 2016. Examining the functioning of a multilayer karst aquifer. The case of Toulon springs. In: Eurokarst 2016. Neuchâtel, pp. 363–370.
Mahler, B.J., Bourgeais, R., 2013. Dissolved oxygen fluctuations in karst spring flow and implications for endemic species: Barton Springs, Edwards aquifer, Texas, USA. J. Hydrol. 505, 291–298.
Mahler, B.J., Musgrove, M., Wong, C.I., Sample, T.L., 2011. Recent (2008-10) water quality in the Burton Springs segment of the Edwards aquifer and its contributing zone, Central Texas, with emphasis on factors affecting nutrients and bacteria. U.S. Geological Survey Scientific Investigations Report 2011–5139. p. 66.
Mahler, B., Valdes, D., Musgrove, M., Massei, N., 2008. Nutrient dynamics as indicators of karst processes: comparison of the chalk aquifer (Normandy, France) and the Edwards aquifer (Texas, USA). J. Contam. Hydrol. 98, 36–49.
Maillet, E., 1905. Essais d'hydraulique souterraine et fluviale (underground and River Hydrology) Hermann, Paris. p. 218.
Mangin, A., 1975. Contribution à l''étude hydrodynamique des aquifères karstiques. Université de Dijon Thèse de Doctorat en Sciences naturelles.
Mangin, A., 1984. Pour une meilleure connaissance des systèmes hydrologiques à partir des analyses corrélatoire et spectrale. J. Hydrol. 67, 25–43.
Massei, N., Dupont, J.P., Mahler, B.J., Laignel, B., Fournier, M., Valdes, S., Ogier, S., 2006. Investigating transport properties and turbidity dynamics of a karst aquifer using correlation, spectral, and wavelet analyses. J. Hydrol. 329, 244–257.
Mayaud, C., Wagner, T., Benischke, R., Birk, S., 2014. Single event time series analysis in a binary karst catchment evaluated using a groundwater model (Lurbach system, Austria). J. Hydrol. 511, 628–639.
Minvielle, S., Lastennet, R., Denis, A., Peyraube, N., 2015. Characterization of karst systems using SIc-PCO_2 method coupled with PCA and frequency distribution analysis. Application to karst systems in the Vaucluse county (Southeastern France). Environ. Earth Sci. 74, 7593–7604.
Moussu, F., 2011. Prise en compte du fonctionnement hydrodynamique dans la modélisation pluie-débit des systèmes karstiques. . Doctorat en Sciences naturelles. Université Pierre et Marie Curie, pp. 202.
Mudarra, M., Andreo, B., 2011. Relative importance of the saturated and the unsaturated zone in the hydrogeological functioning of a karst aquifers: the case of Alta Cadena (Southern Spain). J. Hydrol. 397, 263–280.
Mudarra, M., Andreo, B., Baker, A., 2011. Characterization of dissolved organic matter in karst spring waters using intrinsic fluorescence: relationship with infiltration processes. Sci. Total Environ. 409 (18), 3448–3462.
Musgrove, M., Fahlquist, L., Stanton, G.P., Houston, N.A., Lindgren, R.J., 2011. Hydrogeology, chemical characteristics, and water sources and pathways in the zone of contribution of a public-supply well in San Antonio, Texas. U.S. Geological survey Scientific Investigations Report 2011–5146. p. 194.
Nicolini, E., Rogers, K., Rakowski, D., 2016. Baseline geochemical characterisation of a vulnerable tropical karstic aquifer: Lifou, New Caledonia. J. Hydrol. Reg. Stud. 5, 114–130.
Padilla, A., Pulido-Bosch, A., Mangin, A., 1994. relative importance of baseflow and quickflow from hydrographs of karst springs. Ground Water 32 (2), 267–277.
Padilla, A., Pulido-Bosch, A., 1995. Study of hydrographs of karstic aquifers by means of correlation and cross spectral analysis. J. Hydrol. 168 (1), 73–89.

Palmer, A.N., 2011. Distinction between epigenic and hypogenic maze caves. Geomorphology 134, 9–22.
Panagopoulos, G., Lambrakis, N., 2006. The contribution of time series analysis to the study of the hydrodynamic characteristics of the karst systems: application on two typical karst aquifers of Greece (Trifilia, Almyros Crete). J. Hydrol. 329, 368–376.
Parkhurst, D.L., Appelo, C.A.J., 1999. User's guide to phreeqc (version 2). A computer program for speciation, batch-reaction, one-dimensional transport, and inverse geochemical calculations. US Geological Survey Water-Resources Investigations, Report. pp 99-4259.
Pelissié, T., 1982. Le Causse jurassique de Limogne-en-Quercy: stratigraphie, sédimentologie, structure. Thèse de Doctorat en sciences naturelles. Université Paul Sabatier, Toulouse, pp. 281.
Pélissié, T., Astruc, J.G., 1996. Tectonique synsédimentaire et dissolution d'évaporites dans les dépôts du Jurassique moyen et supérieur des Causses du Quercy. Géol. Fr. 4, 23–32.
Perrin, J., Jeannin, P.Y., Zwahlen, F., 2003. Implications of the spatial variability of infiltration-water chemistry for the investigation of a karst aquifer: a field study at Milandre test site, Swiss Jura. Hydrogeol. J. 11, 673–686.
Perrin, J., Jeannin, P.-Y., Cornaton, F., 2007. The role of tributary mixing in chemical variations at a karst spring, Milandre, Switzerland. J. Hydrol. 332, 152–173.
Peyraube, N., Lastennet, R., Denis, A., 2012. Geochemical evolution of groundwater in the unsaturated zone of a karstic massif, using the PCO_2 – SIc relationship. J. Hydrol. 430–431, 13–24.
Peyraube, N., Lastennet, R., Denis, A., Malaurent, P., 2013. Estimation of epikarst PCO2 using measurements of water $\delta^{13}C_{TDIC}$ cave air P_{CO2} and 1 $\delta^{13}C_{CO2}$. Geochim. Cosmochim. Acta 118, 1–17.
Platel, J.P., 1987. Le Crétacé supérieur de la plate-forme septentrionale du Bassin d'Aquitaine. Université de Bordeaux III, pp. 573 Thèse de Doctorat d'Etat ès Sciences.
Pronk, M., Goldscheider, N., Zopfi, J., 2009. Microbial communities in karst groundwater and their potential use for biomonitoring. Hydrogeol. J. 17, 37–48.
Raeisi, E., Karami, G., 1997. Hydrochemographs of Berghan karst spring as indicators of aquifer characterstics. J. Cave Karst Stud. 59 (3), 112–118.
Rey, J., Cubaynes, R., Faure, P., Hantzpergue, P., Pélissié, T., 1988. Stratigraphie séquentielle et évolution d'une plate-forme carbonatée: le Jurassique du Quercy (Sud-Ouest de la France). Compte Rendu de l'Académie des Sciences Paris 306, série II. pp. 1009–1015.
Rouiller, D., 1987. Etude des systèmes karstiques de la Touvre et de la Lèche. Thèse de Doctorat en Sciences naturelles. Université d'Avignon et des Pays de Vaucluse, pp. 194.
Rowden, R., Liu, H., Libra, R., 2001. Results from the big spring basin water quality monitoring and demonstration projects, Iowa, USA. Hydrogeol. J. 9, 487–497.
Soulios, G., 1991. Contribution à l'étude des courbes de recession des sources karstiques. Exemples du Pays Hellenique. J. Hydrol. 127, 29–42.
Strickland, J.D.H, Parsons, T.R., 1972. A practical Handbook of seawater analysis. Bulletin 167, second ed. p. 328.
Stueber, A., Criss, R., 2005. Origin and transport of discharge chemicals in a karst watershed, Southwestern Illinois. J. Am. Water Resour. Assoc. 41, 267–290.
Tallaksen, L., 1995. A review of baseflow recession analysis. J. Hydrol. 165 (1), 349–370.
Von Stempel, C., 1972. Etude des ressources en eau de la région de Périgueux (Dordogne. Thèse de Doctorat en Sciences naturelles. Université de Bordeaux I, pp. 235.
White, W.B., 1988. Geomorphology and Hydrology of Karst terrains. Oxford University Press, New York, pp. 464.
Worthington, S., Ford, D., 2009. self-organized permeability in carbonate aquifers. Ground Water 47, 326–336.